

STEREO RADARGRAMMETRY USING AIRBORNE SAR IMAGES WITHOUT GCP

Daiki Maruki[†], Shuji Sakai[†], Koichi Ito[†], Takafumi Aoki[†], Jyunpei Uemoto[‡] and Seiho Uratsuka[‡]

[†]Graduate School of Information Sciences, Tohoku University, Japan.

[‡]National Institute of Information and Communications Technology, Japan.

E-mail: maruki@aoki.ecei.tohoku.ac.jp

ABSTRACT

Elevation measurement using Synthetic Aperture Radar (SAR) is one of crucial applications in remote sensing, since the use of SAR in elevation measurement makes it possible to measure a wide range of planar area and not to set any monitoring device on the ground.

Most of conventional methods need Ground Control Points (GCPs) to achieve accurate 3D measurement, where GCP acquisition is a time-consuming and cost-intensive task. Addressing the above problem, this paper proposes a novel stereo radargrammetry method using airborne SAR images without GCP. We define a new sensor model with only parameters provided in SAR image acquisition which derives from the principle of stereo vision. We employ bundle adjustment so as to minimize reprojection errors in 3D measurement, since the proposed sensor model is based on stereo vision. We also employ Phase-Only Correlation (POC), which is a sub-pixel image matching method using phase information obtained by Discrete Fourier Transform (DFT) of given images, to obtain dense and accurate correspondence between two SAR images. Through an experiment using SAR images, we demonstrate that the proposed method exhibits efficient performance of radargrammetry compared with Interferometric SAR (InSAR).

Index Terms— SAR, radargrammetry, sensor model, bundle adjustment, stereo vision

1. INTRODUCTION

Synthetic Aperture Radar (SAR), which is a high-resolution imaging radar mounted on a moving platform such as an aircraft or space-craft, has a significant advantage of acquiring high-resolution radar images with all-day and all-weather imaging capabilities [1]. Elevation measurement using SAR is one of crucial applications in remote sensing, since the use of SAR in elevation measurement makes it possible to measure a wide range of planar area and not to set any monitoring device on the ground. The accurate 3D measurement technique using SAR is indispensable to produce Digital Surface Models (DSMs) of a target area.

Radargrammetry extracts geometric information from radar images using stereoscopy, clinometry, interferometry or polarimetry [1]. Interferometric SAR (InSAR) [2], which is the most popular technique of elevation measurement using SAR, uses the differences in phase between the signals received by two SAR antennas to construct a map of ground surface elevations. Two antennas are set on a single platform in single-pass interferometry, while two SAR images are captured at slightly different orbits in repeat-pass interferometry. Although the accuracy of a DSM measured by InSAR is high, InSAR cannot usually measure the absolute value of elevation, since there is the phase uncertainty. To solve this problem, we must use at least one Ground Control Point (GCP).

The other widely-used technique in radargrammetry is stereoscopy [3], which is similar to the stereo vision technique [4]. The stereoscopic technique needs a sensor model and correspondence between two SAR images. A sensor model describes the geometric relationship between 3D coordinates of a target area and 2D coordinates in the SAR images. Two sensor models, physical sensor model and Rational Function Model (RFM), are used for the stereoscopic technique. The physical sensor model is a complex deterministic model parameterized by the specification of a sensor and the precise orbit information. The use of the physical sensor model takes much computation time to reconstruct 3D coordinates for each pixel in SAR images. The RFM is a simple empirical model represented by ratios of polynomials, which is considered to be an ideal replacement for physical sensor models. Only Rational Polynomial Coefficients (RPC) are required to use the RFM, while multiple GCPs must be used to calibrate RPC in order to achieve accurate 3D measurement comparable with the physical sensor model.

As mentioned above, most of conventional methods for elevation measurement using SAR have to use GCPs such as conversion from phase differences into absolute heights in InSAR and parameter optimization in RFM. Therefore, these methods do not fully utilize the advantage of SAR in elevation measurement. There are a few methods which do not use GCP in elevation measurement [5]. Its measurement accuracy is heavily depending on the accuracy of metadata provided with SAR images.

Addressing the above problems, this paper proposes a novel stereo radargrammetry method using airborne SAR images without GCP. We define a new sensor model with only parameters provided in SAR image acquisition which derives from the principle of stereo vision, resulting in fast computation of 3D measurement. We can employ bundle adjustment [4] which minimizes reprojection errors in 3D measurement, since the proposed sensor model is based on stereo vision. The use of bundle adjustment makes it possible not to use GCP and RPC in stereo radargrammetry. We also employ Phase-Only Correlation (POC) [6, 7], which is a sub-pixel image matching method using phase information obtained by Discrete Fourier Transform (DFT) of given images, to obtain dense and accurate correspondence between two SAR images. Through an experiment using SAR images, we demonstrate that the proposed method exhibits efficient performance of radargrammetry compared with InSAR.

2. 3D GEOMETRIC MODEL OF SAR

In this section, we define a new sensor model determined by only parameters provided in SAR image acquisition. We also derive a theoretical formula to calculate 3D points from two SAR images and the sensor model.

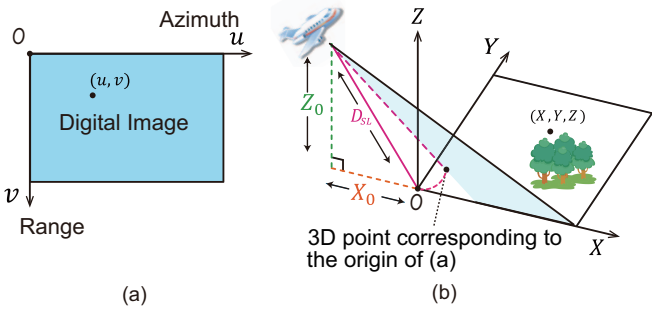


Fig. 1. Definition of coordinate systems: (a) 2D image coordinate system and (b) 3D radar coordinate system.

2.1. Sensor Model and Intrinsic Parameters of SAR

We consider two coordinate systems such as a 2D image coordinate system for an SAR image and a 3D radar coordinate system for a target area as shown in Fig. 1. In the 2D image coordinate system, the coordinate is indicated by (u, v) , the origin O is located at the upper left, and the horizontal axis u and the vertical axis v correspond to the Azimuth direction and the Range direction, respectively. In the 3D radar coordinate system, the coordinate is indicated by (X, Y, Z) , the origin O is located at sea level, and the axes for X , Y and Z correspond to the Range direction, the Azimuth direction and the elevation direction, respectively. Note that the origin in the 2D image coordinate system does not correspond to the origin in the 3D radar coordinate system, except that the origin in the 2D image coordinate system corresponds to sea level.

We define a projection model which describes a relationship between the 3D radar coordinate (X, Y, Z) and the 2D image coordinate (u, v) by

$$u = \alpha_u Y, \quad (1)$$

$$v = \alpha_v (\sqrt{(X_0 + X)^2 + (Z_0 - Z)^2} - D_{SL}), \quad (2)$$

where X_0 is the horizontal distance between the platform and the origin in the 3D radar coordinate system, D_{SL} is the distance between the platform and the origin in the 3D radar coordinate system, Z_0 is the altitude of the platform, and α_u and α_v are constant equal to the inverse of the resolution in the azimuth direction and the slant range direction, respectively. In this paper, we assume that the altitude of the platform, Z_0 , is constant. If the momentarily altitude information is given, we can set the variable altitude Z_0 . D_{SL} is calculated from the time difference between emitting a signal and receiving its echo. X_0 is calculated using Z_0 and D_{SL} by the Pythagorean theorem.

As a result, parameters for the above model are α_u , α_v , Z_0 and D_{SL} , which can be obtained from SAR image acquisition. Eqs. (1) and (2) are considered as a projection model in terms of stereo vision and a sensor model in terms of radargrammetry. In the proposed sensor model, these parameters are called intrinsic parameters of SAR.

2.2. 3D Coordinate Transformation and External Parameters of SAR

We now consider that two SAR images of the same area are acquired from two different orbits, where one orbit is 1 and the other one is 2. Then, the relationship between the 3D coordinate (X, Y, Z) in the orbit 1 and the 3D coordinate (X', Y', Z') in the orbit 2 can be

defined by

$$\begin{bmatrix} X' \\ Y' \\ Z' \end{bmatrix} = \mathbf{R} \begin{bmatrix} X \\ Y \\ Z \end{bmatrix} + \mathbf{t}, \quad (3)$$

where the rotation matrix \mathbf{R} and the translation vector \mathbf{t} are defined by

$$\mathbf{R} = \begin{bmatrix} \cos \phi & -\sin \phi & 0 \\ \sin \phi & \cos \phi & 0 \\ 0 & 0 & 1 \end{bmatrix}, \quad \mathbf{t} = \begin{bmatrix} t_X \\ t_Y \\ 0 \end{bmatrix},$$

respectively. In this paper, the rotation matrix \mathbf{R} and the translation vector \mathbf{t} are called external parameters of SAR.

2.3. Theoretical Formula for 3D Measurement

We derive the theoretical formula for 3D measurement using two SAR images from Eqs. (1), (2) and (3). We consider a coordinate (u, v) on the SAR image from the orbit 1 and a coordinate (u', v') on the SAR image from the orbit 2. From Eqs. (1), (2) and (3), the relationship among a 3D point (X, Y, Z) , (u, v) and (u', v') is defined by

$$u = \alpha_u Y, \quad (4)$$

$$v = \alpha_v (\sqrt{(X_0 + X)^2 + (Z_0 - Z)^2} - D_{SL}), \quad (5)$$

$$u' = \alpha'_u (X \sin \phi + Y \cos \phi + t_Y), \quad (6)$$

$$v' = \alpha'_v (\sqrt{(X'_0 + X \cos \phi - Y \sin \phi + t_X)^2 + (Z'_0 - Z)^2} - D'_{SL}), \quad (7)$$

where α_u , α_v , Z_0 , D_{SL} , and X_0 are parameters for orbit 1 and α'_u , α'_v , Z'_0 , D'_{SL} , and X'_0 are parameters for orbit 2. Assuming that (u, v) and (u', v') are a corresponding point pair, we can calculate the 3D coordinate (X, Y, Z) by solving Eqs. (4)–(7). One approach is to solve all the equations as a least squares problem, while it is very time-consuming to solve the least squares problem for all the measurement points. On the other hand, we empirically confirmed that three of four equations are enough to obtain the 3D coordinate (X, Y, Z) analytically, whose accuracy is comparable to solve the least squares problem of four equations. If the rotation angle ϕ is not zero, we can select Eqs. (4), (5) and (6). Then, the 3D coordinate (X, Y, Z) is given by

$$X = \frac{1}{\sin \phi} \left(\frac{u'}{\alpha'_u} - \frac{u}{\alpha_u} \cos \phi - t_Y \right), \quad (8)$$

$$Y = \frac{u}{\alpha_u}, \quad (9)$$

$$Z = Z_0 - \sqrt{\left(\frac{v}{\alpha_v} + D_{SL} \right)^2 - (X_0 + X)^2}. \quad (10)$$

As mentioned above, our proposed model is represented by intrinsic and external parameters as well as a stereo camera model used in stereo vision [4]. Hence, the use of the proposed stereo SAR model allows us to apply a set of techniques for stereo vision to stereo radargrammetry.

3. 3D MEASUREMENT FROM SAR IMAGES

This section describes a 3D measurement algorithm using the proposed geometric model as mentioned in the previous section. The

proposed algorithm consists of five steps: (i) ground projection, (ii) external parameter estimation, (iii) correspondence matching, (iv) parameter optimization and (v) 3D measurement. The detail of each step is described in the following.

(i) Ground Projection

There is a large deformation between two SAR images acquired in the different orbits, since the spatial resolution of SAR images in the ground range direction is different between orbits and the appearance of SAR images is significantly changed depending on orbits. We have to correct image deformation of SAR images by projecting SAR images onto the X - Y plane by Eq. (1) and (2) so as to perform stable and accurate 3D measurement. In Eq. (2), Z has to be estimated, that is, Z is unknown at first. Hence, we introduce the following procedure to the proposed 3D measurement algorithm. First, assuming $Z = 0$, SAR images are projected onto the X - Y plane by Eq.(1) and (2). Next, we estimate (X, Y, Z) through step (ii)–(v). Using the estimated (X, Y, Z) , SAR images are projected onto the X - Y plane by Eq. (1) and (2). Then, we estimate (X, Y, Z) through step (ii)–(v) again. In the following, the SAR image projected onto the X - Y plane is called the ground range image and the original SAR image before ground projection is called the slant range image.

(ii) External Parameter Estimation

We estimate the rotation angle ϕ and the translational displacement t_X and t_Y , i.e., the external parameters of SAR image, using the latitude and longitude information at the image corners which is included in the metadata. One image is rotated by the estimated rotation angle ϕ to correct image rotation.

(iii) Correspondence Matching

We obtain corresponding point pairs between the ground range images using the correspondence matching method using POC [7]. POC is an image matching technique using the phase components in 2D DFTs of given images and is robust against illumination change and noise [6]. These features of POC are highly effective in matching SAR images. The correspondence matching method using POC employs (i) a coarse-to-fine strategy using image pyramids for robust correspondence search and (ii) a sub-pixel translational displacement estimation method using POC for local block matching [7]. Corresponding point pairs on the slant range image is obtained by applying the inverse transformation of rotation correction and ground projection to the corresponding point pairs on the ground range images.

(iv) Parameter Optimization

We optimize the intrinsic and external parameters in nonlinear optimization by minimizing reprojection error using bundle adjustment [4], which is known as one of the optimization techniques used in stereo vision, since these parameters include errors during the process of SAR image acquisition. Let \mathbf{P} be intrinsic and external parameters to be optimized and $\mathbf{m}_{1,i} = (u_1, v_1)_i$ and $\mathbf{m}_{2,i} = (u_2, v_2)_i$ be the i -th corresponding point pair between the slant range images of orbits 1 and 2, respectively, where $1 \leq i \leq N$. Bundle adjustment minimized cost function $E(\mathbf{P})$ defined by

$$E(\mathbf{P}) = \sum_{i=1}^N (\|\mathbf{m}_{1,i} - \mathbf{m}_{\text{rep}1,i}(\mathbf{P})\|^2 + \|\mathbf{m}_{2,i} - \mathbf{m}_{\text{rep}2,i}(\mathbf{P})\|^2), \quad (11)$$

where $\mathbf{m}_{\text{rep}1,i}(\mathbf{P})$ and $\mathbf{m}_{\text{rep}2,i}(\mathbf{P})$ indicate the coordinates obtained by projecting a 3D point onto the slant range images of the orbits 1 and 2, respectively, and the 3D point is calculated from $\mathbf{m}_{1,i}$, $\mathbf{m}_{2,i}$ and \mathbf{P} . We employ the Levenberg-Marquardt (LM) method, which is one of the nonlinear least-squares optimization

Table 1. Specification of SAR image acquisition used in the experiment.

Path	Altitude Z_0 [m]	Look angle θ [deg.]	1/resolution [pixel/m]	
			α_u	α_v
1	9,193	35.29	4	5.34
2	9,191	36.41	4	5.34

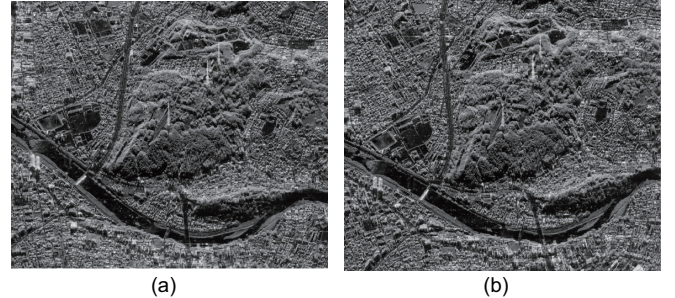


Fig. 2. SAR images acquired from the area in Sendai, Japan: (a) SAR image of orbit 1 and (b) SAR image of orbit 2, where the images are acquired at August 22, 2014.

methods, in the above nonlinear optimization processes. The proposed geometric model for SAR images is not necessary to obtain accurate metadata of SAR images, since we can use bundle adjustment to optimize intrinsic and external parameters, i.e., metadata of SAR images. This is a strong advantage of using our proposed model.

(v) 3D Measurement

Finally, we estimate 3D points using optimized intrinsic and external parameters and Eqs. (8), (9) and (10).

4. EXPERIMENTS AND DISCUSSION

This section describes performance evaluation of the proposed method. To evaluate the accuracy of the proposed method, we employ the Digital Surface Model (DSM) as a ground truth, which is acquired by an airplane laser measurement system and whose measurement accuracy is 0.25m.

4.1. Dataset

Two SAR images are acquired with about 10° -intersection angle between two orbits by Pi-SAR2, which is the airborne X band SAR developed by National Institute of Information and Communications Technology (NICT), Japan. Table 1 shows the specification of SAR image acquisition and Fig.2 shows two SAR images used in the experiment. Intrinsic parameters for two SAR images are almost the same as shown in Table 1. The size of SAR images is $8,000 \times 6,886$ pixels (Fig.2 (a)) and $8,000 \times 6,741$ pixels (Fig.2 (b)). The target area is located at $N38^\circ 14'22''$ and $E140^\circ 52'39''$, where is Sendai, Japan, and includes a mountain with forest, urban area and river. The size of the target area is $2\text{km} \times 2\text{km}$.

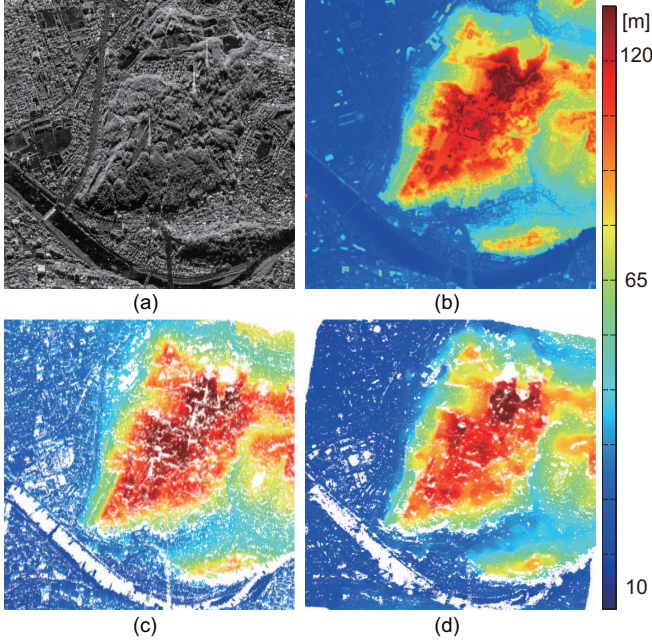


Fig. 3. Generated elevation maps: (a) input SAR image, (b) the ground truth (DSM), (c) InSAR and (d) the proposed method.

Table 2. Summary of experimental results: RMSE, MAE and the number of 3D points. Note that outliers having error of more than 20m are excluded.

	RMSE	MAE	# of 3D points
InSAR	4.70m	3.45m	1,616,234
Proposed	4.49m	3.19m	2,048,194

4.2. Experiment

We reconstruct 3D points from two SAR images using the proposed method. We also obtain 3D points using InSAR for the purpose of performance comparison, which is acquired by the interferometric function of Pi-SAR2. We align the 3D points and DSM using the Iterative Closest Point (ICP) algorithm [8] and evaluate the residual error of elevation. The SAR images with $8,000 \times 6,800$ pixels are transformed to the image with $2,000 \times 2,000$ pixels, where one pixel corresponds to 1m. The window size of image matching for POC is 128×128 pixels. If the peak value of the POC function and the reprojection error are below threshold, we remove the point as an outlier, where the threshold for POC and reprojection error is 0.1 and 2, respectively. Correspondence matching is performed in all the pixels of $1,800 \times 1,800$ -pixel area, which is a common area between two SAR images.

4.3. Experimental Results

Fig. 3 shows elevation maps generated by DSM, InSAR and the proposed method. The color value corresponds to the elevation and the white point indicates an unmeasurable point, i.e., no data. The appearance of InSAR is similar to that of DSM, although there are

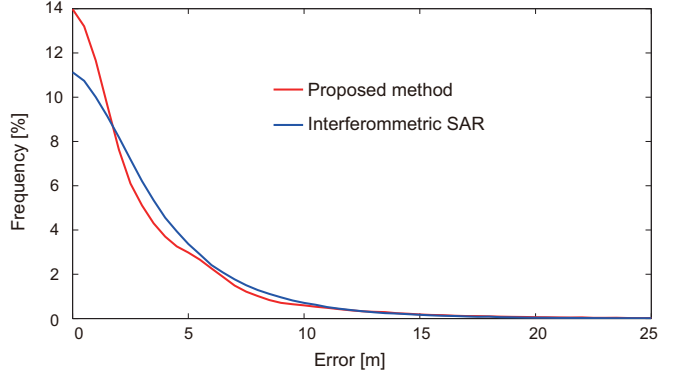


Fig. 4. Error histogram for InSAR and the proposed method.

a lot of unmeasurable points. On the other hand, the appearance of the proposed method is almost the same as that of DSM and unmeasurable points is less than InSAR. Fig. 4 shows the error histogram of InSAR and the proposed method. The frequency of the proposed method is higher than that of InSAR within the area below 2m errors, in other words, the elevation map generated by the proposed method has more accurate 3D points than that by InSAR. Table 2 shows the summary of experimental results such as Root Mean Squared Error (RMSE), Mean Absolute Error (MAE) and the number of 3D points. Note that errors in Table 2 are calculated using 3D points having error of less than 20m, since a 3D point having error of more than 20m is obviously an outlier and such points are less than 1% of all the 3D points for both methods.

As observed above, the accuracy of the elevation map generated by the proposed method, which does not need GCP, is higher than that by InSAR, which usually requires at least one GCP.

5. CONCLUSION

This paper proposed a novel stereo radargrammetry method using airborne SAR images. We define a new sensor model with only parameters provided in SAR image acquisition which derives from the principle of stereo vision. We employ bundle adjustment [4] so as to minimize reprojection errors in 3D measurement. We also employ Phase-Only Correlation (POC) [6, 7] to obtain dense and accurate correspondence between two SAR images. Through an experiment using SAR images, we demonstrated that the proposed method exhibits efficient performance of radargrammetry compared with InSAR.

6. REFERENCES

- [1] P.-G.P. Ho, *Geoscience and Remote Sensing*, InTech, Oct. 2009.
- [2] P. A. Rosen, S. Hensley, I. R. Joughin, Fuk K. Li, S. N. Madsen, E. Rodriguez, and Richard M. Goldstein, “Synthetic aperture radar interferometry,” *Proc. IEEE*, vol. 88, no. 3, pp. 333–382, Mar. 2000.
- [3] P. Capaldo, M. Crespi, F. Fratarcangeli, A. Nascetti, and F. Pieralice, “High-resolution SAR radargrammetry: A first application with COSMO-SkyMed spotlight imagery,” *IEEE Geosci. Remote Sens. Lett.*, vol. 8, no. 6, pp. 1100–1104, Nov. 2011.

- [4] R. Szeliski, *Computer Vision: Algorithms and Applications*, Springer-Verlag New York Inc., 2010.
- [5] T. Toutin, “Radarsat-2 DSM generation with new hybrid, deterministic, and empirical geometric modeling without GCP,” *IEEE Trans. Geosci. Remote Sens.*, vol. 50, no. 5, pp. 2049–2055, May 2012.
- [6] K. Takita, T. Aoki, Y. Sasaki, T. Higuchi, and K. Kobayashi, “High-accuracy subpixel image registration based on phase-only correlation,” *IEICE Trans. Fundamentals*, vol. E86-A, no. 8, pp. 1925–1934, Aug. 2003.
- [7] K. Takita, M. A. Muquit, T. Aoki, and T. Higuchi, “A subpixel correspondence search technique for computer vision applications,” *IEICE Trans. Fundamentals*, vol. E87-A, no. 8, pp. 1913–1923, Aug. 2004.
- [8] Z. Zhang, “Iterative point matching for registration of free-form curves and surfaces,” *Int'l J. Computer Vision*, vol. 13, no. 2, pp. 119–152, Oct. 1994.